Linking excess order to co-solvent aggregation in solvent mixtures

Silvia Imberti

Published version information

Citation: S Imberti. "Linking excess order to co-solvent aggregation in solvent mixtures." Molecular Physics, Soper Special Issue (2019).

DOI: 10.1080/00268976.2019.1649483

This is an Accepted Manuscript of an article published by Taylor & Francis in Molecular Physics on 03-08-19, available online: http://www.tandfonline.com/

Linking excess order to co-solvent aggregation in solvent mixtures

Silvia Imberti*

UKRI-STFC, ISIS neutron and muon source, Rutherford Appleton Laboratory, Harwell Campus, Chilton, Didcot, OX11 0QX, United Kingdom

E-mail: silvia.imberti@stfc.ac.uk

Abstract

Small amphiphilic molecules dissolved in alcohol-water mixtures have been seen to have a tendency to aggregate. Here we present a thorough neutron diffraction experiment, aided by H/D isotopic substitution and empirical potential structure refinement simulations of four mixtures of tert-butyl alcohol (x_t=0.03 molar) in methanol and water (x_m=0.27, 0.54, 0.73, 1.0 molar). The tert-butyl alcohol is found to segregate in the methanol rich regions at all concentrations; at x_m=0.27 the mixture is found to be a bi-percolating mixture, with water forming one interconnected cluster, and methanol and tert-butyl alcohol (apolar-apolar) forming another. At the same x_m=0.27 concentration, tert-butyl alcohol molecules become closer each other at this concentration, forming more dimers than at the other concentrations, and even trimers. Results are discussed in terms of the ability of water molecules to form flexible tetrahedral networks.

Introduction

A number of polymers that are commonly soluble both in water and alcohol, display a dramatic collapse when 10-20 molar % of alcohol is added to the polymer/water system.[1] This phenomenon is known as co-non-solvency and despite having been extensively studied by the polymers community, it still sparks heated debate in literature. According to Mukherji et al.[2] the alcohol is able to preferentially bind distal monomers thus guiding the polymer to collapse, and the entire process would therefore be enthalpically favoured. It is worth noting though that co-non-solvency has been called upon to explain the stabilisation of the folded state of proteins by the addition of a small amount of alcohol or other osmolytes. Indeed, at higher alcohol concentration the proteins become denatured, and in a similar way the polymers become solvated again. When Mochizuki et al. set out to understand the "minimal conditions required in order to observe co-non-solvency",[3] they focused their attention onto smaller molecules. In a Molecular Dynamics (MD) study, Mochizuki and Koga have found that small hydrophobic molecules such as methane in water/methanol mixtures have a tendency to aggregate more at certain concentrations than at 2 others.[4] In a further study, including spectroscopic data as well as MD, Mochizuki et al. have found that co-non-solvency behaviour appears even for small amphiphilic molecules dissolved in water/methanol mixtures.[3] In particular, they found that methanol molecules preferentially solvate dimers of tert-butyl alcohol (TBA), as opposed to monomers. In the conclusions, Mochizuki et al. state that "to further understand the molecular origin of co-non-solvency, it would be useful to further explore inhomogeneous mixing in the MeOH/water solvent itself".

The inhomogeneous mixing of alcohol/water mixtures has indeed been extensively studied by neutron scattering by Soper et al. since 2002.[5] The problem of the causes of co-non-solvency therefore intersects and has implications for the long-standing debate on the hydrophobic effect and the observed excess order in alcohol/water mixtures.[6] In these 17 years of publications and particularly in a very recent re-visitation of the topic,[7] the full power of combining neutron diffraction with isotopic substitution (NDIS)[8] and a simulation

method developed specifically for the interpretation of total scattering data from molecular liquids, the empirical potential structure refinement (EPSR)[9] has been exploited. The main findings can be summarised as:

1. there is no sign of a water structure enhancement (in the form of straighter, shorter hydrogen bonds) *around* the hydrophobic groups of the alcohol in the alcohol water/mixture;[5]

2. there is an approximate concentration range (0.27-0.54 MeOH molar fraction x_m) where the solvent mixture undergoes a quite dramatic change in its structure, which becomes a bi-percolating mixture;[10]

3. outside of these range, only one of the two components is percolating and the other components forms small clusters that are not interconnected;[11]

4. the alcohol/alcohol structuring is mainly sterically driven (it is not affected by the removal of Coulombic interaction between the molecules in the EPSR simulation);[7]

5. the water/water interaction is affected by the removal of Coulombic interaction in the EPSR simulation;[7]

6. the strength of hydrogens bonds among water molecules (and not around the hydrophobic groups) is therefore enhanced at certain concentrations in the alcohol water mixture;[11]

With the present study, the powerful combination of neutron diffraction with isotopic substitution and EPSR simulation has been applied to studying the aggregation and solvation of an amphiphilic compound (TBA) in a water/methanol mixtures at various concentrations.

Table 1: Details of the four tert-butyl alcohol (TBA), methyl alcohol (MeOH) and water mixtures measured in this work. Atom labels used in the following pages are: CC_{MeOH} for the central carbon, CM_{MeOH} on the methyl group, O_{MeOH} and H_{MeOH} on the hydroxyl group for the tertiary butanol; C_{MeOH} on the methyl group, O_{MeOH} and H_{MeOH} on the hydroxyl group for the methanol. Methyl hydrogens had a separate label in the simulations but they do not appear in the results presented in the following.

Concentration	TBA	MeOH	W
(a)	0.03	0.27	0.73
(b)	0.03	0.54	0.46
(c)	0.03	0.73	0.27
(d)	0.03	1	0

Table 2: H/D composition for each concentration.

H/D composition	TBA $(CH_3)_3$	TBA OH	MeOH CH_3	MeOH OH	W OH_2
x.1	D	D	D	D	D
x.2	H	D	H	D	D
x.3	HD	D	HD	D	D
x.4	D	H	D	H	H
x.5	D	HD	D	HD	HD
x.6	H	H	H	H	H
x.7	HD	HD	HD	HD	HD

Experiment

Neutron diffraction enhanced by hydrogen/deuterium isotopic substitution (NDIS)[8] has been used to study the solutions detailed in table 1. The experimental data obtained by these techniques were then used to constrain a Monte Carlo based simulation in a method known as Empirical Potential Structure Refinement (EPSR).[9] The neutron experiments have been performed at the SANDALS diffractometer (ISIS spallation neutron and muon source, Rutherford Appleton Laboratory, United Kingdom). SANDALS is a total scattering neutron diffractometer optimized for the study of hydrogen containing liquids and amorphous samples. The physical quantity measured by the diffractometer is the differential scattering cross section $d\Sigma/d\Omega$ as a function of the exchanged wave vector Q (defined as the modulus of the difference between the incident and the scattered neutron wave vectors). Through the basic theory of neutron scattering, it is possible to relate this quantity to the static structure factor $F(Q)$, which is the Fourier transform of the site-site radial distribution function (RDF) $g(r)$ (see for example Hansen and McDonald[12]). The latter contains the information about the correlation between the positions of two atoms in the system at a given moment.

In the case of a multicomponent system, it can be shown[12] that the structure factor is a linear combination of the partial structure factors $S_{\alpha\beta}(Q)$ in the following way:

$$F(Q) = \sum_{\alpha\beta\geq\alpha} (2 - \delta_{\alpha\beta}) c_\alpha c_\beta b_\alpha b_\beta S_{\alpha\beta}(Q) \tag{1}$$

where α and β are two atom types present in the system, $\delta_{\alpha\beta}$ is the Kronecker delta function, c is their concentration and b their scattering length.[13] Since the scattering length b varies from one isotope to another, the shape of the measured function $F(Q)$ can vary quite dramatically with changing the isotopes involved. In particular, by substituting ^{1}H (b =-3.740 fm) with ^{2}H (b =6.671 fm), it is possible to highlight H-X correlations, where X is a non-substituted atom (e.g. oxygen).

The samples were contained in flat plate TiZr cans, both sample and wall thickness are

1mm. The standard corrections and normalizations have been applied to the data through the set of programs gathered under the graphical interface *GudrunN*. The theoretical background to the operations performed by the program are described in reference programs for correcting raw neutron and x-ray diffraction data to differential scattering cross section. [14]

Four mixture have been measured[1]:

- the concentration of TBA is maintained constant and low (x_t=0.03 molar)
- the concentrations of the water/methanol mixture is the same as the ones investigated by Soper e al. in his excess order study, [11] i.e. methanol fraction x_m= 0.27, 0.54, 0.73, 1 (see table 1).

For each concentration, 7 different combinations of deuteriated mixtures have been measured; The H/D compositions have been chosen to highlight selectively the hydrophilic and hydrophobic interaction within the solutions (see table 2). The data that support the findings of this study are openly available[2] in ISIS Data Journal at http://doi.org/10.5286/ISIS.E.97954563, reference number RB1800065. For each concentration, one simulation which simultaneously incorporates the contribution from all seven patterns has been performed using the EPSR method.

Table 3: Details of the EPSR boxes used in this work. More details, such as the reference potential used to initiate the simulations are provided in the Supporting Information.

Concentration	TBA	MeOH	W	density	box side
	no. molecules			atom/Å^3	Å
(a)	150	1350	3650	0.0918	61.45
(b)	150	2700	2300	0.0922	27.49
(c)	150	3650	1350	0.0913	67.60
(d)	150	5000	0	0.0898	71.08

[1]Please note that pure TBA and TBA in water have previously been investigated via neutron diffraction with isotopic substitution by Bowron et al. [15 16]

[2]The release date is: Tue Jun 29 09:00:00 BST 2021

Data modelling

Models of the experimental data have been constructed using the Empirical Potential Structure Refinement (EPSR) program.[17] The method has been described in detail elsewhere (see Soper[9] and references therein) and therefore only a brief summary will be given here. The algorithm is based on a classical Monte Carlo simulation of the molecular system under study at fixed concentration and density, and employs an iterative algorithm that aims at building an atomistic three dimensional model consistent with the scattering data. The simulation proceeds through a number of stages. In the first stage the simulation follows the standard Monte Carlo algorithm for simulations of molecular structures, based on a pairwise reference potential (Lennard-Jones plus Coulomb). In the following stage a perturbation potential is determined from the difference between the calculated and experimental structure factors. The simulation box is equilibrated with the reference plus empirical potential and a new empirical potential is calculated and added to the previous one. This iterative process drives the model into agreement with the data. Once agreement is reached between the experimental and model structure factors, the final stage of the procedure is undertaken and structural information is collected in the form of ensemble averages. Each simulation box contained more than 5000 molecules and was accumulated for a minimum of 10000 configurations.

Results

The comparison between experimental and simulated structure factors can be inspected in Figure 1. From the simulation boxes the site-site pair distribution functions (PDF) or radial distribution functions g(r)s (RDFs) have been extracted, containing information about the most likely, nearest-neighbour positions for all the atomic pairs in the simulation box. Coordination numbers (CNs) have been calculated for all the oxygen-oxygen combinations (see table 5). Atom labels used in the following pages are: CC_{MeOH} for the central carbon, CM_{MeOH} on the methyl group, O_{MeOH} and H_{MeOH} on the hydroxyl group for the tertiary

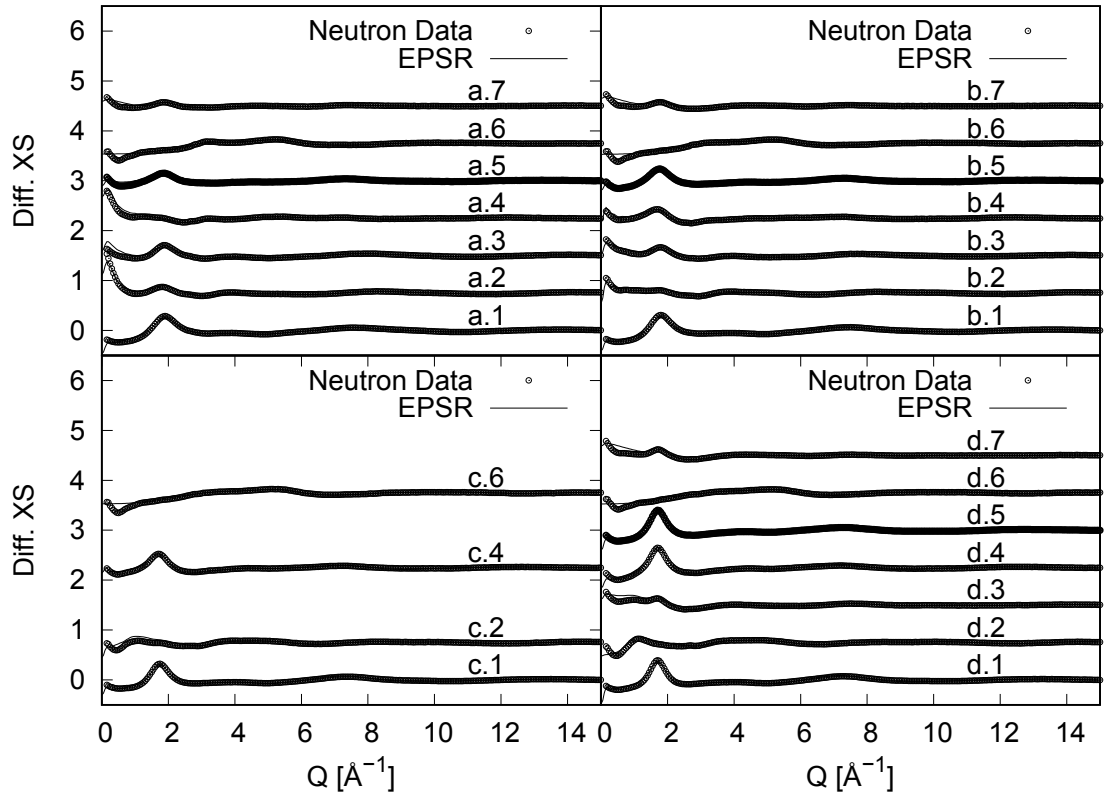

Figure 1: Calculated (line) and experimental (symbols) differential cross-section (XS) data for 7 distinct isotopic substitutions (table 2 at concentrations (a) x_m=0.27, (b) x_m=0.54, (c) x_m=0.73 and (d) x_m=1.0. For concentration (c), only 4 out of 7 H/D substitutions have been measured due to a technical issue. Curves are shifted vertically for clarity. Units of the differential cross sections are barns/atom/sr.

butanol; C_{MeOH} on the methyl group, O_{MeOH} and H_{MeOH} on the hydroxyl group for the methanol. Methyl hydrogens had a separate label in the simulations but they do not appear in the results presented in the following.

Firstly, the solvent-solvent structure is analysed to determine whether the solutions retain the clustering behaviour observed previously in methanol-water mixtures[7] even after the addition of a small amount of TBA. Indeed the solutions present percolation both for the hydrogen-bonded water component and for apolar contacts in the methanol component at the intermediate concentrations of (a) x_m=0.27 (see figure 2) and (b) x_m=0.54. Plot of the clustering at the concentrations x_m=0.54-1.00 are reported in the Supporting Information. In terms of coordination numbers (table 5 in the Supporting information), the number of water-water, methanol-water contacts decreases with increasing methanol concentration, and the opposite trend is observed for the methanol-methanol and water-methanol contacts, as expected.

We therefore proceed to answer the first question that we have set out to investigate: **is there an increased aggregation of TBA molecules at certain concentrations of the solutions?** The answer is positive as evidenced when performing a "cluster" analysis on TBA, shown in figure 3: at concentrations (a) x_m=0.27 and (b) x_m=0.54 TBA has greater tendency to form dimers than at the other concentrations and at x_m=0.27 it even forms trimers. this result is quite remarkable considering that TBA is overall quite diluted, and at any of the solvent compositions studied here there are always sufficient water and methanol molecules to solvate fully the TBA molecules. Therefore one wouldn't expect its aggregation to be greatly influenced by a variation in the concentration of the co-(non?)-solvents.

The following question we may ask is what is the driving force in this aggregation process? Specifically, is there a monotonic trend with concentration in the tendency for TBA to form hydrogen bonds , g(r) O_{TBA}-O_{TBA} and O_{TBA}-H_{TBA}) or to form hydrophobic contacts (g(r) CM_{TBA}-CM_{TBA} and CC_{TBA}-CC_{TBA})? Indeed (see figure 4), there is a tendency for solution (a) x_m=0.27 and (b) x_m=0.54 to form more hydrophobic contacts and for (a) x_m=0.27 to

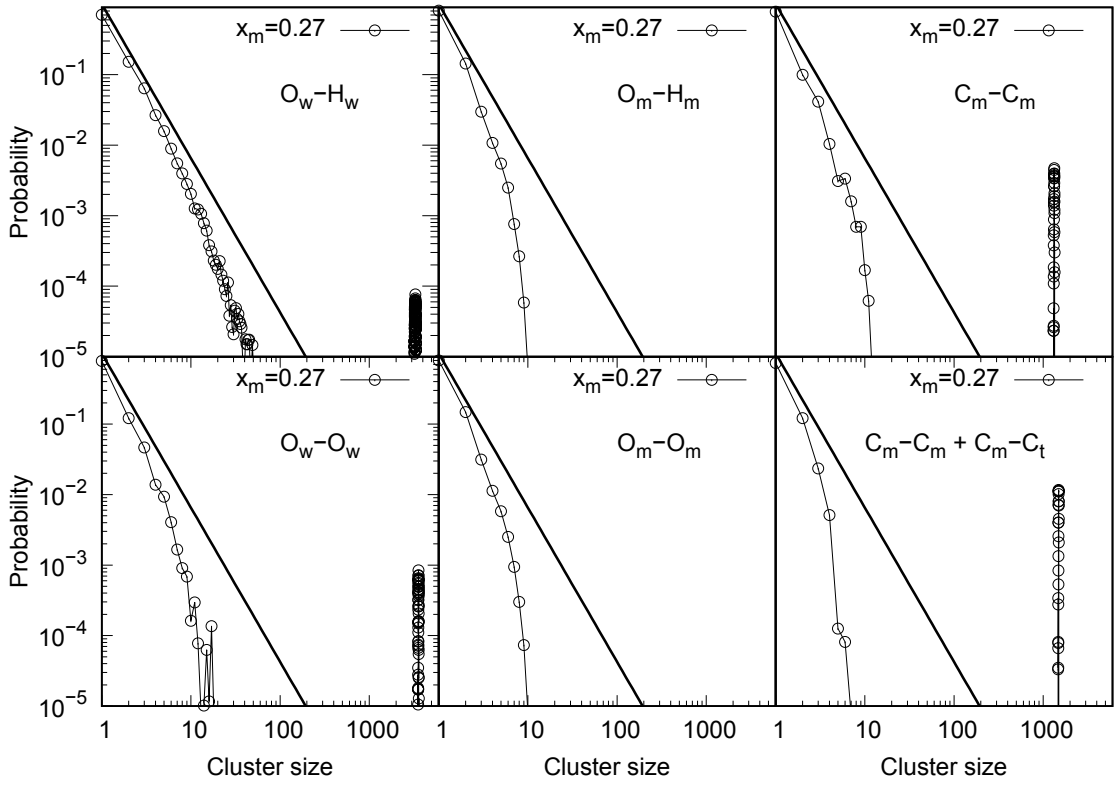

Figure 2: Water-water and methanol-methanol cluster size distribution in ternary TBA-water-methanol solutions for methanol molar concentration x_m=0.27 (The other concentrations are available in the Supporting information, figure 10. Water-water HB connectivity (left) with the following cutoff: O_w-H_w at 2.35 Å, O_w-O_w at 3.6 Å. Methanol-methanol connectivity (middle and right) with the following cutoff: O_m-H_m at 2.35 Å, O_m-O_m at 3.2 Å, C_m-C_m at 5.5 Å. In he bottom right figure the cluster formed by MeOH-MeOH and MeOH-TBA apolar connection is calculated, with C_m-C_m at 5.5 Åand C_m-C_t at 5.1 Å. The thick line shows the predicted distribution $x^{-2.186}$ at the percolation threshold.[18]

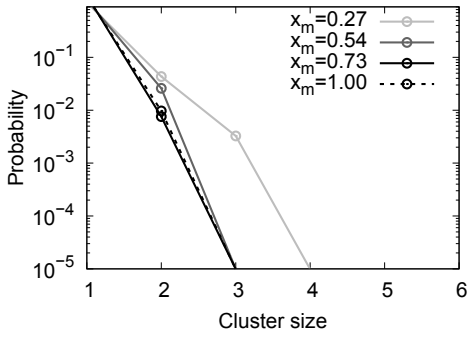

Figure 3: Cluster size distribution in ternary TBA-water-methanol solutions at all concentrations. O_{TBA}-O_{TBA} connectivity with a cutoff at 3.5 Å. At concentrations (a) x_m=0.27 and (b) x_m=0.54 TBA has greater tendency to form dimers, and at x_m=0.27 it even forms trimers.

form more hydrogen bonds. It is admittedly a small effect on a lowly weighted partial RDF, and further experiments at higher concentration and with a different type of molecule in solution are called for, in order to increase the weighting of TBA-TBA interactions in the experimental data.

At the current concentration, a more reliable indication of what could be driving the TBA molecules together could be provided by an analysis of the solvent-solvent and TBA-solvent g(r)s, as these have a stronger weight in constraining the simulations.

In figure 5, the oxygen-oxygen RDFs for all possible combinations in our solution are presented, including the already partly described solvent-solvent ones. The figure present two vertical lines, as a guidance for the eyes, at 2.75 and 4.3Å, i.e. the usually observed distance for, respectively, hydrogen bond (HB) between two water molecules and between three water molecules that are bonded via HB to each other. The position of the second peak in the RDFs with respect to the vertical line is particularly useful, and has been used in the literature for describing the presence of an extended network of hydrogen bonds in the liquid. Starting from the top, the OW-OW RDF shows that the first peak is at the same position as it is for pure water. The first peak for O_{MeOH}-OW and O_{TBA}-OW hydrogen bonds is shorter, whilst the one for hydrogen bonds between the amphiphilic molecules, i.e. O_{MeOH}-O_{MeOH}, O_{MeOH}-O_{TBA} and O_{TBA}-O_{TBA} is even shorter and therefore stronger. It

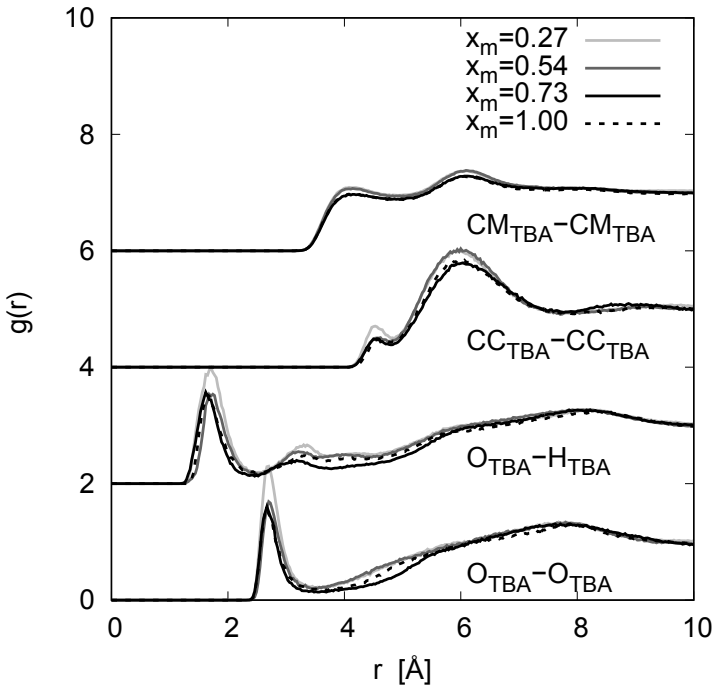

Figure 4: Radial distribution function for hydrogen bonds and apolar contacts between TBA molecules as a function of concentration. The trend with concentration should be read together with the coordination numbers in table 5

seems, and it is slightly counter-intuitive, that when a non-polar group is also present on the molecule, the polar sides of the molecules form shorter bonds. This mean that they are somehow less hindered to doing so, most likely because they do not have to satisfy other hydrogen bonds at the same time.

It is interesting to notice that all of the oxygen-oxygen g(r)s have the same concentration trend (except for the already discussed TBA-TBA one); for the first peak, the intensity is decreasing when the water concentration decreases, while for the second peak the lines cross over and the peak intensity increases in inverse correlation to the water content. When the concentration of the components is variable, the peak intensity on its own is not significant, and the whole area multiplied by the atomic fraction c_β of each single component, or coordination number (CN) of atom β around atom α, is the relevant quantity:

$$N_{\alpha\beta} = 4\pi\rho c_\beta \int_0^{r_{min}} r^2 g_{\alpha\beta}(r) dr. \tag{2}$$

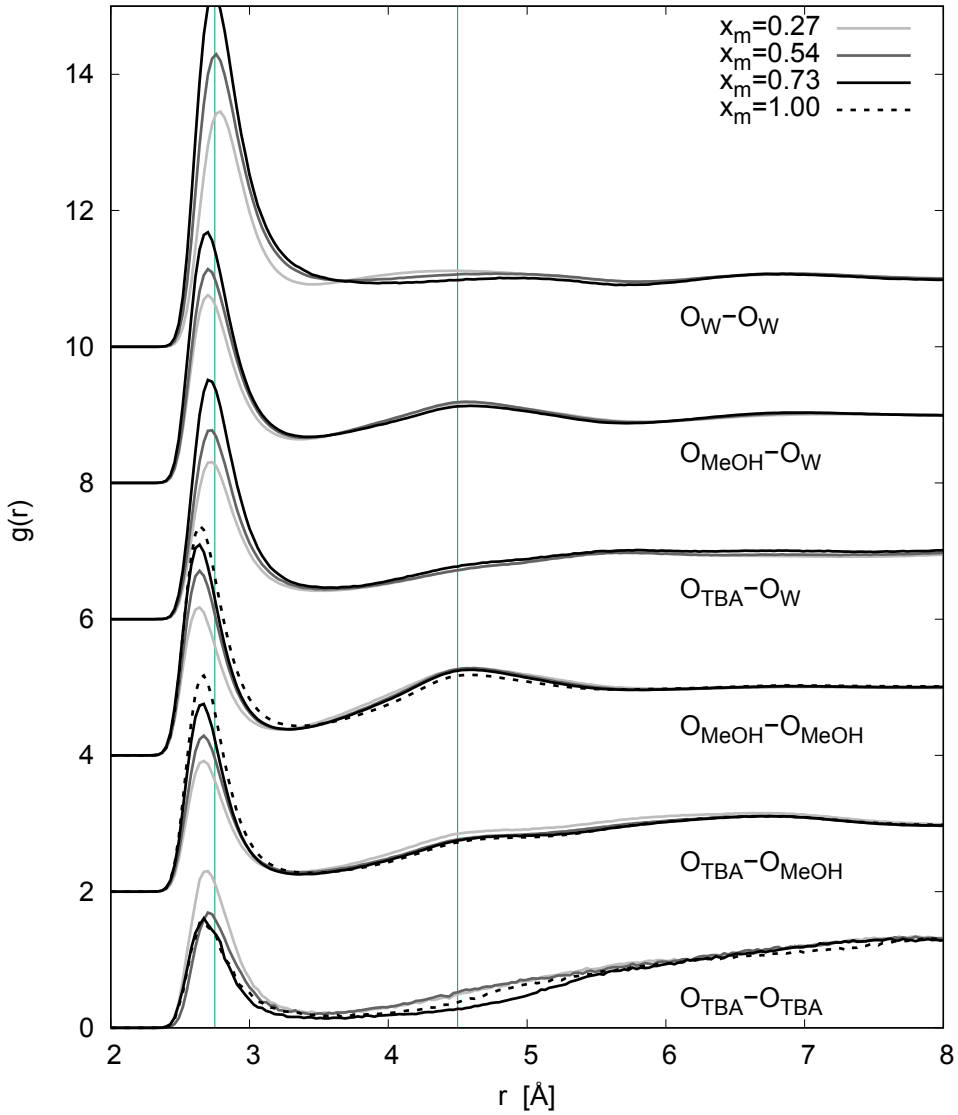

Figure 5: Radial distribution function between oxygen pairs in the mixtures as a function of concentration. The vertical bars correspond to the peak positions of the first and second shells in pure water. The trend with concentration should be read together with the coordination numbers in table 5

The full set of calculate CNs is available in table 5. Overall the behaviour is the expected one insofar as where the β atom is the water oxygen O_w, the CN decrease with water concentration, while the opposite happens when the β atom is the methanol oxygen O_m. More interestingly, the latter increase does not compensate for the previous decrease, meaning that the number of hydrogen bonds that methanol makes does not compensate for the ones lost when the water concentration decreases. The reason is because methanol only has two sites available for hydrogen bonding, one donor hydroxyl-hydrogen and one acceptor hydroxyl-oxygen, while water has four (two donors, two acceptors). Overall, the total number of hydrogen bonds decreases with decreasing water content, as evidenced in a stacked histogram plot in figure 6.

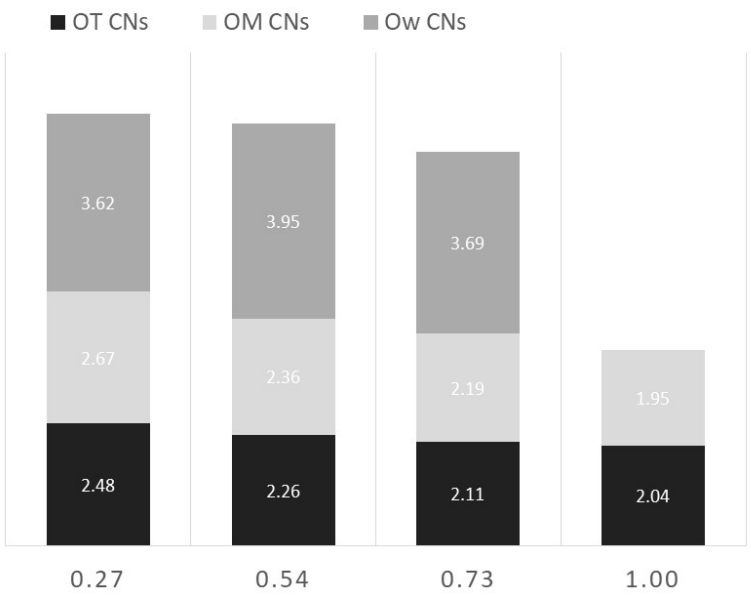

Figure 6: Oxygen-oxygen coordination numbers in stacked histogram representation, corresponding to the first peaks in figure 5. The total coordination number around water, methanol and TBA are presented as a function of methanol concentration; the individual numbers used for this plot are reported in detail in table 5. The total number of hydrogen bonds decreases with decreasing water content.

The fact that at the highest water content the overall number of hydrogen bonds is higher can help explain why at this concentration all of the oxygen-oxygen RDFs show slightly higher

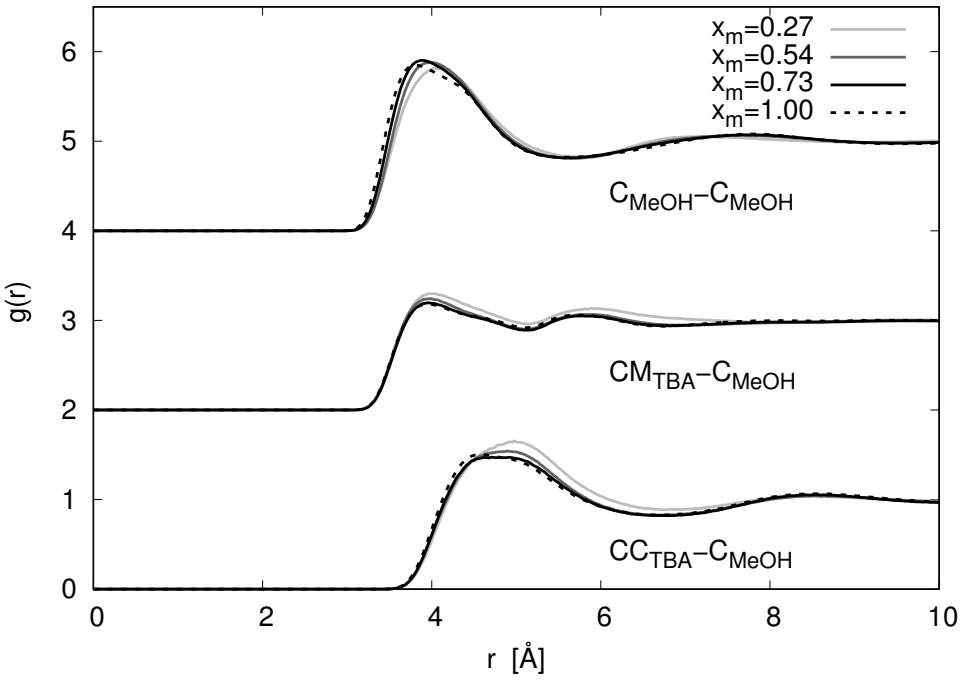

Figure 7: Radial distribution function for apolar contacts between TBA and methanol interactions as a function of concentration.

intensity on the second peak. This peak is traditionally associated with the presence of an extended network of hydrogen bonds.

We observe that:

1. the second peak of the OW-OW RDF is moving with water concentrations. The hydrogen bonded network in water is therefore changing and adapting in response to the changing concentration. None of the other peaks shows the same amount of variation.

2. the O_{MeOH}-O_{MeOH} correlations and the O_{MeOH}-OW ones do present a second peak that hardly moves with the concentration. The position of the second peak in these pairs is determined as a consequence of the position of the first and is not a driver for changes with concentration in our solutions;

3. the O_{TBA}-O_{TBA} second peak is absent or at least it is moved to farther distances, as expected given the very low concentration of TBA molecules in solutions. We may

have TBA-TBA contacts but we do not have an extended network, as already seen in figure 3;

4. O_{TBA}-OW does not have a second peak, while at the same time the O_{TBA}-O_{MeOH} does, thus indicating that the **TBA molecules are mainly residing in methanol rich domains**;

In a more detailed analysis of the OW-OW RDF, at the highest water concentration (a), the second peak is slightly compressed towards the first one - a feature often seen in electrolytic aqueous solutions[19] or wherever a considerable amount of water is engaged in the solvation shell of another specie. On the other hand at the remaining two concentrations, where water is less than 50 molar%, the second peak is flattened/moved towards higher distances, indicating a lower degree of long range order.

Overall, from this geometrical analysis, it can be envisaged the presence of two competing effects at play in the solvent mixture: (i) the requirement to satisfy all of the hydrogen bonds available sites, a job that is mainly left to water molecules, that are small and flexible as they form slightly longer HBs among themselves and with the solutes and (ii) the requirement to accommodate and increasing number of very weakly interacting polar groups (so weakly, that in the scale that we can detect with the combination of neutrons and EPSR simulations, it doesn't make any difference if charges are present or not[7]).

Water adapts and modifies its extended network in order to comply with both these requirements, with signature in the movement of the second peak of the OW-OW RDF. This long description was necessary to prepare the ground and build anticipation for the next question: **How is this water rearrangement impacting on the distance among apolar sites of the methanol and TBA molecules?** The carbon-carbon RDFs in figure 7 show that the C_{MeOH}-C_{MeOH} peak is hardly affected by the changing concentrations, with possibly a decrease in intensity at the highest water concentration. There is some potential effect on the apolar interaction between TBA and methanol. Overall there is a marginal enhancement of apolar contacts between TBA and methanol, alongside with that

of the TBA-TBA ones (described previously), but not of the methanol-methanol ones, at the highest water concentrations. On the contrary, the polar TBA-TBA interaction displays a most significant enhancement at the highest water concentration (figure 4). It is worth noting that although a systematic study of this aspect has not been performed a this stage, this peak appears to have grown in the simulation with the number of configurations accumulating, indicating a possible collective self-aggregation phenomenon.

Conclusions

In conclusion, it is certainly found that TBA prefers to reside in methanol rich domains, and that TBA-TBA interactions are stronger at the highest water concentration studies here (x_m=0.27), the same concentration at which the bipercolating behaviour sets in for these water/methanol mixtures. Water molecules are adapting their extended network constantly to the changing concentration. At concentrations of water above 50 molar % the extended network of hydrogen bonds in water behaves like it always does in the presence of a protic solvent: it shrinks and compresses. When a critical concentration is reached (roughly below 50 molar % for the sake of this discussion) maintaining an extended network is not possible anymore. As a consequence the network becomes much more open, with a shift of the second peak of the OW-OW RDF. At this stage, many other molecules become part of the water HB network. Due to steric hindrance and lower polarisability, the methanol molecules do not have the same flexibility in forming networks. The HB made by methanol molecules does not change greatly with varying concentration. Overall, the solution has more hydrogen bonds when more water molecules are present (See figure 6). Methanol accepts 2.5 HBs at the highest water concentration, as opposed to 2 HBs when only methanol is present. Most of these "excess" HBs are provided by water molecules. The much more adaptable (polarisable and less bulky) water molecules satisfy the maximum number of hydrogen bonds by adapting the geometry of their network. This has an impact on the energetic balance of the solution.

While the solution with the highest water content (a) shows some overstructuring of the water molecules, solutions (b) and (c) have a more disordered water network. Hence a non trivial enthalpic/entropic contribution is at play within these solutions, which should not be overlooked when trying to predict the solvation of polymers.

In conclusion, it is necessary to combine detailed neutron diffraction experiments as well as theoretical thermodynamic calculations in order to disentangle this veritable conundrum. Experiments at higher concentrations of TBA, as well as including a different solvent mixture are ongoing.

Supporting Information Available

Details about experimental and computational technique. Structure factors (experimental and calculated via EPSR). Complete plots of site-site radial distribution functions.

Acknowledgements

I acknowledge the ISIS Facility Access Panel for allocating beamtime RB1800065. I would also like to thank Prof. Maria Antonietta Ricci for useful suggestions on the present manuscript as well as continuous encouragement over the years. I warmly thank Dr Alex Hannon for careful proof-reading of this manuscript. Finally, I would like to thank Prof. Alan Soper for welcoming me into the Disordered Materials group back in 2007, and then always listening and patiently answering neutrons or EPSR questions.

References

(1) Mukherji, D.; Marques, C. M.; Stuehn, T.; Kremer, K. *Journal of Chemical Physics* **2015**,

(2) Mukherji, D.; Wagner, M.; Watson, M. D.; Winzen, S.; de Oliveira, T. E.; Marques, C. M.; Kremer, K. *Soft Matter* **2016**, *12*, 7995–8003.

(3) Mochizuki, K.; Sumi, T.; Koga, K. *Phys. Chem. Chem. Phys.* **2017**, *19*, 23915–23918.

(4) Mochizuki, K.; Koga, K. *Phys. Chem. Chem. Phys.* **2016**, *18*, 16188–16195.

(5) Dixit, S.; Crain, J.; Poon, W. C. K.; Finney, J. L.; Soper, A. K. *Nature* **2002**, *416*, 829–832.

(6) Chandler, D. *Nature* **2005**, *437*, 640–647.

(7) Lenton, S.; Rhys, N. H.; Towey, J. J.; Soper, A. K.; Dougan, L. *J. Phys. Chem. B* **2018**, *122*, 34.

(8) Finney, J. L.; Soper, A. K. *Chemical Society Reviews* **1994**, *23*, 1 – 10.

(9) Soper, A. K. *Molecular Simulation* **2012**, *38*, 1171–1185.

(10) Dougan, L.; Bates, S. P.; Hargreaves, R.; Fox, J. P.; Crain, J.; Finney, J. L.; Réat, V.; Soper, A. K. *The Journal of Chemical Physics* **2004**, *121*, 6456–6462.

(11) Soper, A. K.; Dougan, L.; Crain, J.; Finney, J. L. *Journal of Physical Chemistry B* **2006**, *110*, 3472–3476.

(12) Hansen, J.-P.; McDonald, I. *Theory of Simple Liquids*; Academic Press: Amsterdam, 2006.

(13) Sears, V. F. *Neutron News* **1992**, *3*, 26.

(14) Soper, A. *RAL Technical Report* **2011**, 2011–013.

(15) Bowron, D. T.; Finney, J. L.; Soper", A. K. *Mol. Phys.* **1998**, *93*, 531 – 543.

(16) Bowron, D. T.; Finney, J. L.; Soper, A. K. *J. Phys. Chem. B* **1998**, *102 (18)*, 3551 – 3563.

(17) Soper, A. K. *RAL Technical Report* **2011**, 2011–012.

(18) Jan, N. *Physica A: Statistical Mechanics and its Applications* **1999**, *266*, 72 – 75.

(19) Imberti, S.; Botti, A.; Bruni, F.; Cappa, G.; Ricci, M.; Soper, A. *Journal of Chemical Physics* **2005**, *122*.

Supporting Information

Table 4: Reference potential for the EPSR simulations, composed by Lennard-Jones parameters plus Coulomb charges.

	ϵ [kJ/mol]	σ [Å]	q [e]	
CC	0.2093	3.80	0.2970	Central C (TBA)
CT	0.6069	3.96	0.0000	Methyl C (TBA)
OT	0.7116	3.07	-0.7280	Hydroxyl O (TBA)
HT	0.0000	1.35	0.0000	Methyl H (TBA)
HOT	0.0000	0.00	0.4310	Hydroxyl H (TBA)
CM	0.3900	3.70	0.2970	Methyl C (MeOH)
OM	0.5850	3.08	-0.7280	Hydroxyl O (MeOH)
M	0.0650	1.80	0.0000	Methyl H (MeOH)
HOM	0.0000	0.00	0.4310	Hydroxyl H (MeOH)
OW	0.6500	3.17	-0.8476	Water O
HW	0.0000	0.00	0.4238	Water H

Table 5: Coordination numbers for all the oxygen-oxygen pairs in the mixtures. For the labels refer to table 4.

site α	site β	r_{max}	CN x_m=0.27	CN x_m=0.54	CN x_m=0.73	CN x_m=1.00
OT	OT	3.40	0.07±0.26	0.05±0.22	0.01±0.12	0.01±0.12
OT	OM	3.40	0.46±0.64	1.03±0.76	1.38±0.77	2.02±0.56
OT	OW	3.50	1.95±0.87	1.18±0.89	0.72±0.76	-
	total OT		2.48	2.26	2.11	2.04
OM	OM	3.30	0.47±0.63	1.00±0.78	1.38±0.77	1.89±0.64
OM	OT	3.40	0.05±0.22	0.06±0.24	0.06±0.24	0.06±0.24
OM	OW	3.40	2.15±0.94	1.30±0.91	0.76±0.77	-
	total OM		2.67	2.36	2.19	1.95
OW	OW	3.4,3.8,3.9	2.74±1.17	2.35±1.34	1.56±1.21	-
OW	OT	3.50	0.08±0.28	0.08±0.28	0.08±0.28	-
OW	OM	3.40	0.79±0.82	1.52±0.98	2.04±1.00	-
	total OW		3.62	3.95	3.69	-

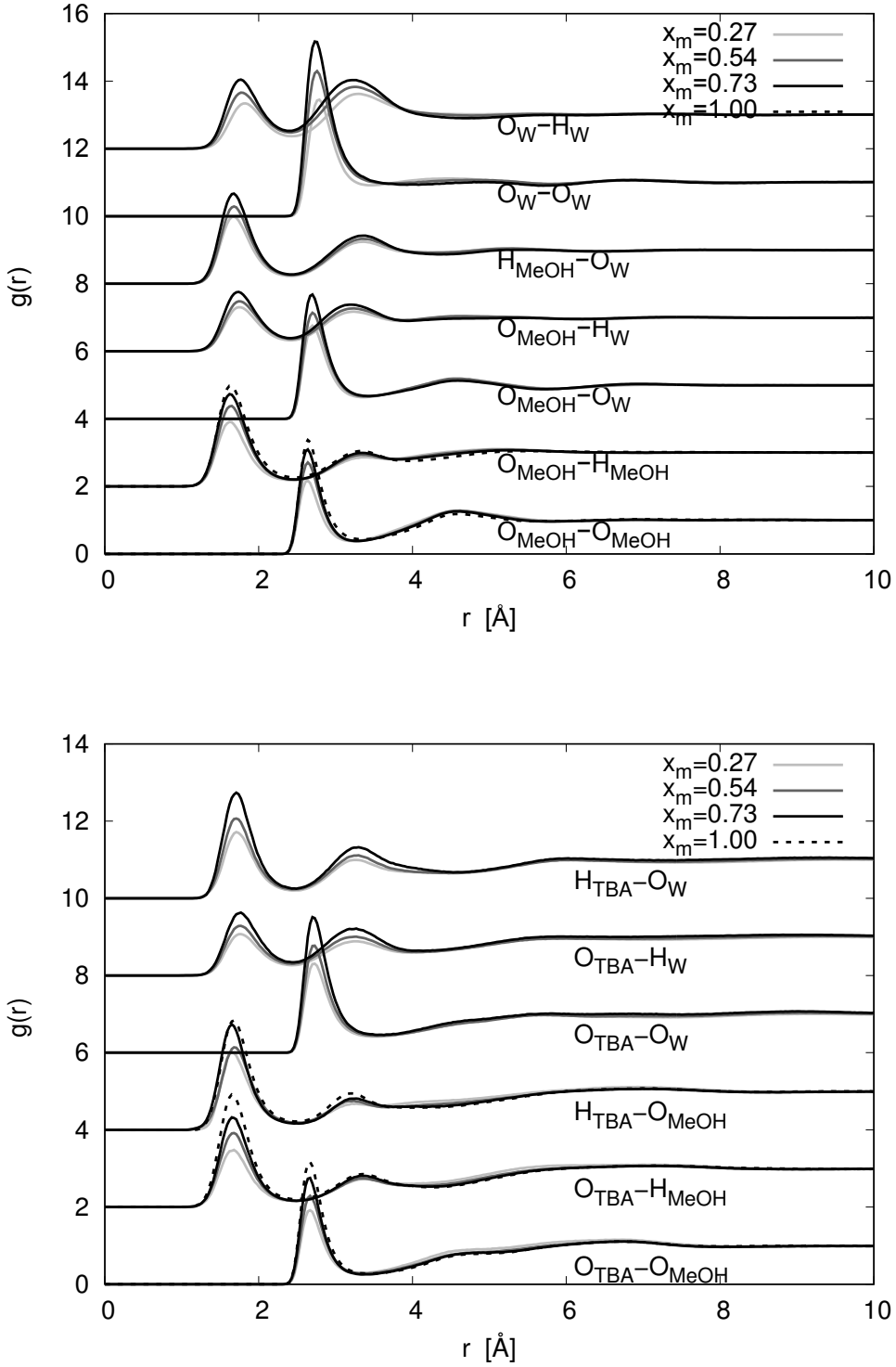

Figure 8: Radial distribution function for hydrogen bonds between TBA and the solvent mixture, highlighting both the TBA-water and TBA-methanol interactions as a function of concentration. The trend with concentration should be read together with the coordination numbers in table 5

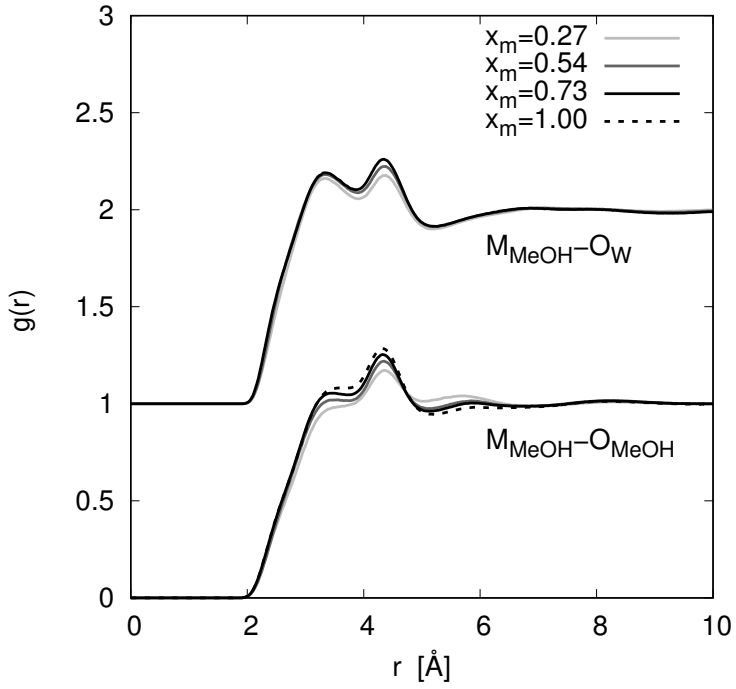

Figure 9: Radial distribution function between methyl-hydrogen to oxygen pairs in the mixtures as a function of concentration.

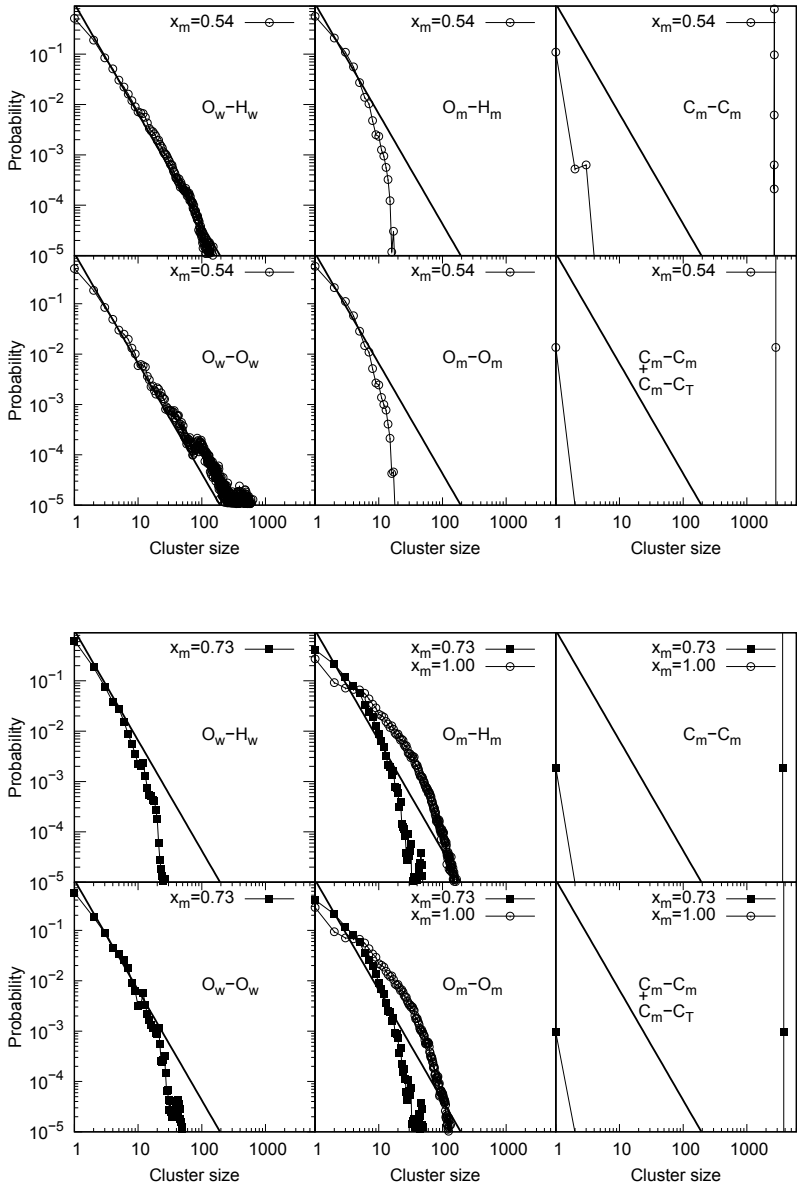

Figure 10: Water-water and methanol-methanol cluster size distribution in ternary TBA-water-methanol solutions. Water-water HB connectivity (left) with the following cutoff: O_w-H_w at 2.35 Å, O_w-O_w at 3.6 Å. Methanol-methanol connectivity (middle and right) with the following cutoff: O_m-H_m at 2.35 Å, O_m-O_m at 3.2 Å, C_m-C_m at 5.5 Å. In he bottom right figure the cluster formed by MeOH-MeOH and MeOH-TBA apolar connection is calculated, with C_m-C_m at 5.5 Åand C_m-C_t at 5.1 Å. The thick line shows the predicted distribution $x^{-2.186}$ at the percolation threshold.[18]